

Co-localized line-field confocal optical coherence tomography and confocal Raman microspectroscopy for three-dimensional high-resolution morphological and molecular characterization of skin tissues *ex vivo*: supplement

LÉNA WASZCZUK,^{1,2,*} JONAS OGIEN,²  JEAN-LUC PERROT,³ AND ARNAUD DUBOIS^{1,2}

¹Université Paris-Saclay, Institut d'Optique Graduate School, CNRS, Laboratoire Charles Fabry, Palaiseau 91127, France

²DAMAE Medical, Paris 75013, France

³University Hospital of Saint-Etienne, Department of Dermatology, 42055 Saint-Etienne, France

*lena.waszczuk@universite-paris-saclay.fr

This supplement published with Optica Publishing Group on 25 March 2022 by The Authors under the terms of the [Creative Commons Attribution 4.0 License](https://creativecommons.org/licenses/by/4.0/) in the format provided by the authors and unedited. Further distribution of this work must maintain attribution to the author(s) and the published article's title, journal citation, and DOI.

Supplement DOI: <https://doi.org/10.6084/m9.figshare.19317548>

Parent Article DOI: <https://doi.org/10.1364/BOE.450993>

Co-localized line-field confocal optical coherence tomography and confocal Raman microspectroscopy for three-dimensional high-resolution morphological and molecular characterization of skin tissues *ex vivo*: supplemental document

1. ILLUSTRATIONS OF THE CO-LOCALIZATION SET-UP

Pictures of the set-up used for co-localized LC-OCT and CRM acquisitions are given in Fig. [S1](#).

2. CALIBRATION PROCESS FOR LC-OCT/CRM CO-LOCALIZATION

The principle of co-localization relies on a coordinate-based calibration between the two XYZ stages placed under the LC-OCT and the CRM devices. The calibration process is schematically described in Fig. [S2](#).

3. EVALUATION OF THE CO-LOCALIZATION ACCURACY

Bead n°	1	2	3	4	5	6	7	8	9	10
Positioning error along X (μm)	0	0	20	10	10	10	10	10	20	10
Positioning error along Y (μm)	0	0	10	0	10	10	10	0	20	0
Positioning error along Z (μm)	10	10	10	10	0	0	10	10	0	0

Table S1. Evaluation of the co-localization accuracy. For 10 TiO_2 beads included in the calibration sample and targeted with LC-OCT, we measured the positioning error defined as the deviation between the theoretical XYZ position of the CRM stage given by the calibration and the actual XYZ position of the stage to effectively target the center of the bead with CRM. A maximum deviation of 20 μm and 10 μm was measured in X/Y and Z respectively.

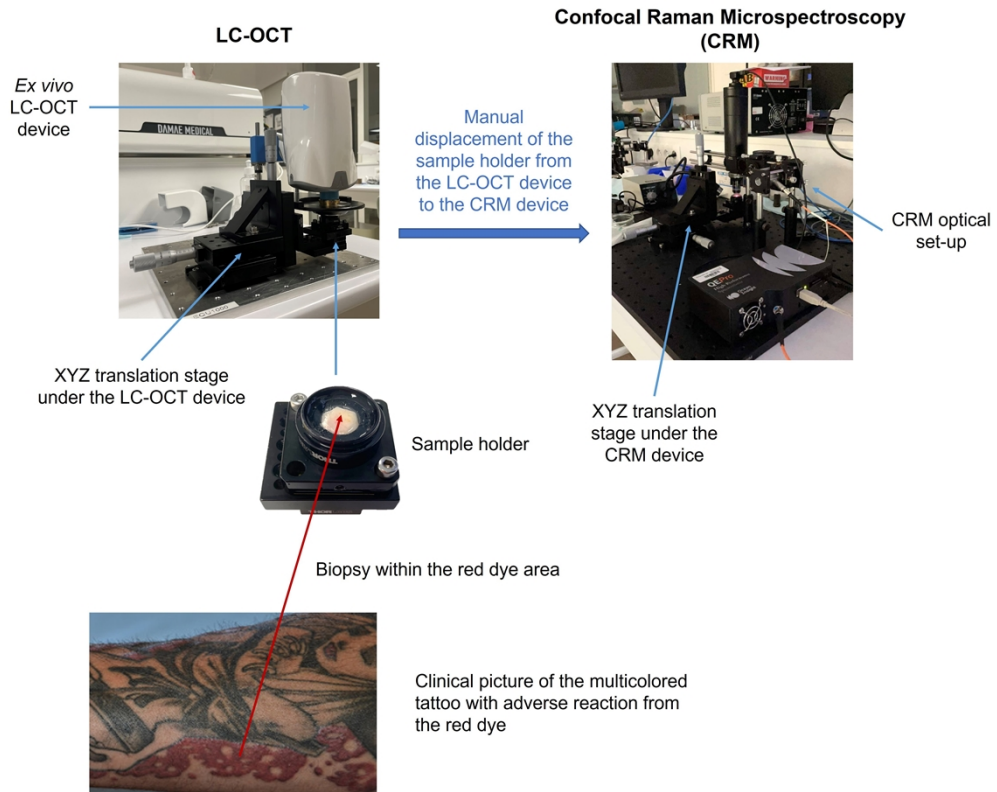


Fig. S1. Pictures of the set-up used for LC-OCT and CRM co-localized acquisitions. Identical XYZ translation stages are placed under the LC-OCT and CRM devices. To perform colocalization experiments, the skin sample is introduced in a sample holder. The sample holder is successively placed on the LC-OCT stage and on the CRM stage. Points of interest (POIs) in the sample are identified from 3D LC-OCT images. A calibration of the XYZ coordinates of the stages under each system, performed prior to experiments, allows to target these same POIs using the CRM system and acquire their Raman spectra. Samples of tattooed skin were characterized with LC-OCT and CRM using this set-up. Samples included a biopsy taken from the red dye area of multicolored tattoo with adverse reaction, as shown in the clinical image.

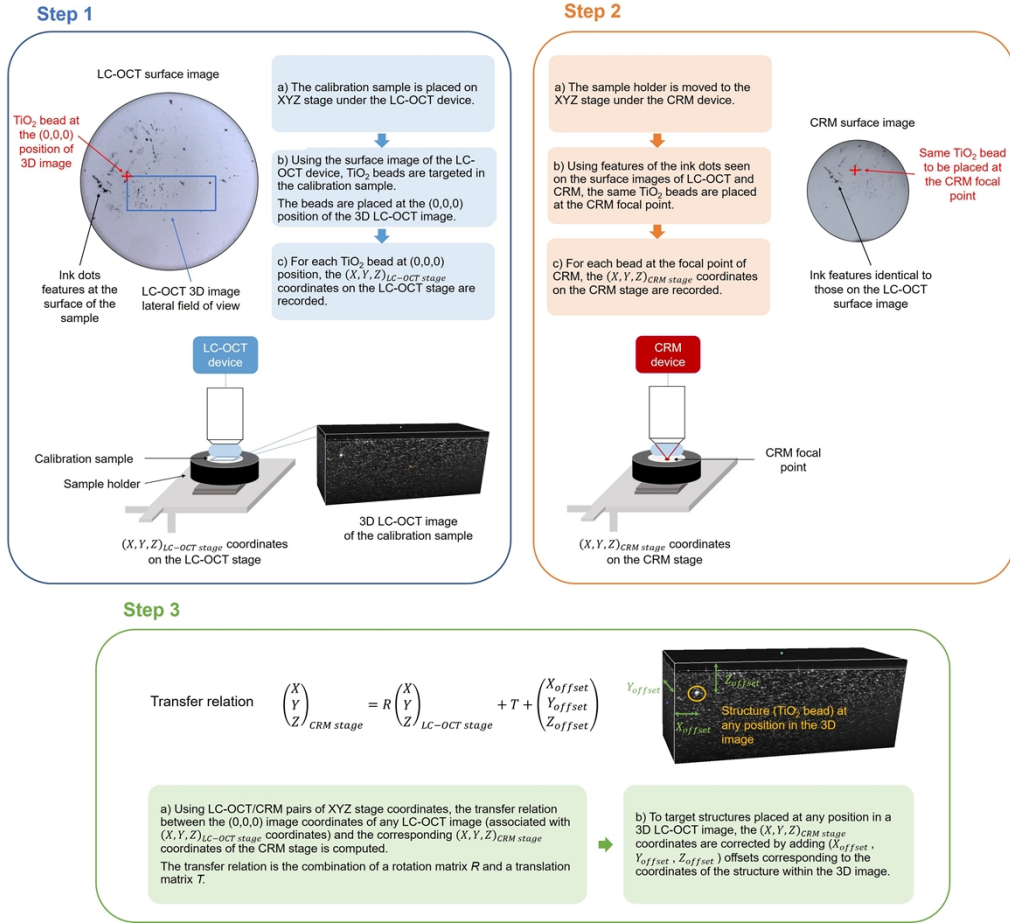


Fig. S2. Diagram describing the calibration process required to perform LC-OCT/CRM colocalized acquisitions. Calibration aims at finding the transfer relation between the coordinates of any POI in a 3D LC-OCT image (acquired for given $(X, Y, Z)_{LC-OCT\ stage}$ coordinates on the LC-OCT stage) and the $(X, Y, Z)_{CRM\ stage}$ coordinates on the CRM stage that makes this POI positioned at the CRM focal point. This transfer relation can be expressed by a combination of a rotation matrix *R*, a translation matrix *T* and correction offsets *X_{offset}*, *Y_{offset}* and *Z_{offset}*. Calibration consists in three main manual steps and is performed using a calibration sample composed of polydimethylsiloxane including titanium dioxide TiO₂ beads.